ARL-TR-7838 ● SEP 2016

Molecular Beam Epitaxy Growth and Characterization of Thin Layers of Semiconductor Tin

by P Folkes, P Taylor, C Rong, B Nichols, H Hier, and M Neupane

Approved for public release; distribution unlimited.

NOTICES

Disclaimers

The findings in this report are not to be construed as an official Department of the Army position unless so designated by other authorized documents.

Citation of manufacturer's or trade names does not constitute an official endorsement or approval of the use thereof.

Destroy this report when it is no longer needed. Do not return it to the originator.

ARL-TR-7838 ● SEP 2016

Molecular Beam Epitaxy Growth and Characterization of Thin Layers of Semiconductor Tin

by P Folkes, P Taylor, C Rong, B Nichols, H Hier, and M Neupane
Sensors Electron and Devices Directorate, ARL

Approved for public release; distribution unlimited.

REPORT DOCUMENTATION PAGE			*Form Approved* *OMB No. 0704-0188*

Public reporting burden for this collection of information is estimated to average 1 hour per response, including the time for reviewing instructions, searching existing data sources, gathering and maintaining the data needed, and completing and reviewing the collection information. Send comments regarding this burden estimate or any other aspect of this collection of information, including suggestions for reducing the burden, to Department of Defense, Washington Headquarters Services, Directorate for Information Operations and Reports (0704-0188), 1215 Jefferson Davis Highway, Suite 1204, Arlington, VA 22202-4302. Respondents should be aware that notwithstanding any other provision of law, no person shall be subject to any penalty for failing to comply with a collection of information if it does not display a currently valid OMB control number.

PLEASE DO NOT RETURN YOUR FORM TO THE ABOVE ADDRESS.

1. REPORT DATE *(DD-MM-YYYY)*	**2. REPORT TYPE**	**3. DATES COVERED (From - To)**
September 2016	Technical Report	

4. TITLE AND SUBTITLE	**5a. CONTRACT NUMBER**
Molecular Beam Epitaxy Growth and Characterization of Thin Layers of Semiconductor Tin	
	5b. GRANT NUMBER
	5c. PROGRAM ELEMENT NUMBER
6. AUTHOR(S)	**5d. PROJECT NUMBER**
P Folkes, P Taylor, C Rong, B Nichols, H Hier, and M Neupane	
	5e. TASK NUMBER
	5f. WORK UNIT NUMBER
7. PERFORMING ORGANIZATION NAME(S) AND ADDRESS(ES)	**8. PERFORMING ORGANIZATION REPORT NUMBER**
US Army Research Laboratory ATTN: RDRL-SED-E 2800 Powder Mill Road Adelphi, MD 20783-1138	ARL-TR-7838
9. SPONSORING/MONITORING AGENCY NAME(S) AND ADDRESS(ES)	**10. SPONSOR/MONITOR'S ACRONYM(S)**
	11. SPONSOR/MONITOR'S REPORT NUMBER(S)

12. DISTRIBUTION/AVAILABILITY STATEMENT

Approved for public release; distribution unlimited.

13. SUPPLEMENTARY NOTES

14. ABSTRACT

Thin layers of single-crystal, epitaxial semiconductor tin (α-Sn) were grown by molecular beam epitaxy (MBE) on cadmium telluride (CdTe) substrates. X-ray diffraction and Raman scattering measurements confirm that the thin layers of α-Sn are slightly strained, which supports theoretical prediction that α-Sn is a 3-D topological insulator (TI). Future studies will aim at the growth of α-Sn with improved transport characteristics using high-quality CdTe buffer layers, studies of the 3-D TI characteristics of α-Sn, and the MBE growth of stanene.

15. SUBJECT TERMS

semiconductor, single-crystal epitaxial tin, α-Sn, MBE, molecular beam epitaxy, topological insulator, single crystal

16. SECURITY CLASSIFICATION OF:			**17. LIMITATION OF ABSTRACT**	**18. NUMBER OF PAGES**	**19a. NAME OF RESPONSIBLE PERSON**
					Patrick Folkes
a. REPORT	**b. ABSTRACT**	**c. THIS PAGE**			**19b. TELEPHONE NUMBER (Include area code)**
Unclassified	Unclassified	Unclassified	UU	16	301-394-1042

Standard Form 298 (Rev. 8/98)
Prescribed by ANSI Std. Z39.18

Contents

List of Figures iv

1. Introduction 1

2. Experimental 1

3. Results 3

4. Conclusion 7

5. References 8

List of Symbols, Abbreviations, and Acronyms 9

Distribution List 10

Approved for public release; distribution unlimited.

List of Figures

Fig. 1 (Left) Schematic layout of MBE for the growth of α-Sn/CdTe (111) and (right) the reflection high-energy electron diffraction (RHEED) pattern confirming epitaxial growth of α-Sn on CdTe (111) at 253 K ..2

Fig. 2 X-ray diffraction spectrum from 20-nm-thick epitaxial α-Sn/CdTe (111) 4

Fig. 3 Photograph of the surface of a 1000-Å (left) and 200-Å (right) layer of α-Sn 4

Fig. 4 Color-coded AFM map of the surface of a 200-Å layer of α-Sn 5

Fig. 5 Raman scattering spectra from a 1000-Å layer of α-Sn....6

Fig. 6 Raman scattering spectrum from a 200-Å layer of α-Sn 7

Approved for public release; distribution unlimited.

1. Introduction

In recent years, there has been strong research interest in semiconductor tin (α-Sn) due to theoretical predictions that, depending on its thickness, α-Sn is a 3-D or 2-D topological insulator (TI). Three-dimensional TIs are electronic materials that have a bulk bandgap and gapless conducting surface states that are protected by the topological and symmetry characteristics of their bandstructure.[1] One of the fundamental characteristics of 3-D TIs is the occurrence of gapless surface states where the conduction band and the valence band touch each other at distinct points in the Brillouin zone, called Dirac points. Near those points the electronic energy-momentum dispersion is similar to the linear dispersion of massless relativistic electrons described by the Dirac equation.[1] Two-dimensional TIs exhibit spin-filtered ballistic transport in edge channels where the up-spins propagate in one direction, while the down-spins propagate in the opposite direction at low temperatures and elastic backscattering is suppressed in the absence of magnetic impurities. These results suggest the possible realization of room-temperature electrical conduction without dissipation in the edge channels of 2-D TIs with a large bandgap and applications in TI-based, energy-efficient devices.[2]

Recent theory[3] has predicted that a monolayer tin film (stanene) is a 2-D TI with a bulk bandgap up to 0.3 eV, which is sufficiently large for practical applications at room temperature. This theoretical prediction has not been observed, because the growth of 2-D tin film has not been achieved. Bulk single-crystal α-Sn is a zero-bandgap semiconductor that is stable at temperatures lower than 286 K and undergoes a phase transition at 286 K to metallic tin (β-Sn), the stable tin allotrope at temperatures above 286 K.[4]

High-quality, single-crystal layers of slightly strained α-Sn that are predicted to be 3-D TIs[5,6] were grown by molecular beam epitaxy (MBE)[7] on indium antimonide and cadmium telluride (CdTe) substrates at room temperature. The MBE-grown layers of α-Sn are stabilized by the substrate and undergo a transition to β-Sn at around 390 K. Raman scattering from single-crystal and polycrystalline bulk tin has been reported[8,9] In this report, we present results of a study of the MBE growth and Raman scattering characterization of thin layers of α-Sn.

2. Experimental

The MBE growth of α-Sn was accomplished at the unusually low substrate temperature of –20 C. The schematic layout of the MBE is shown on the left panel of Fig. 1. High-purity elemental tin metal was used for the growth of α-Sn. The only other source material used is elemental Te, which was only used during a brief

Approved for public release; distribution unlimited.

thermal cleaning of the CdTe substrate. Before loading into the MBE, the CdTe substrates were etched using a dilute bromine-methanol solution, which leaves a somewhat protective Te-rich surface.[10] Once the substrates were loaded into the MBE, they were thermally cleaned to remove the protective Te-rich layer by heating the substrate above 450 °C.

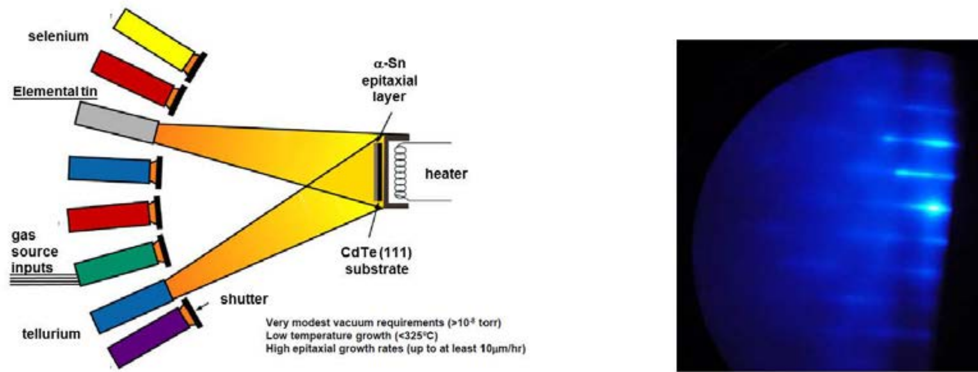

Fig. 1 (Left) Schematic layout of MBE for the growth of α-Sn/CdTe (111) and (right) the reflection high-energy electron diffraction (RHEED) pattern confirming epitaxial growth of α-Sn on CdTe (111) at 253 K

A small overpressure of Te in the form of Te dimers (Te_2) was maintained on the surface during the high-temperature heating to preserve proper 1:1 Cd-to-Te stoichiometry. After the tellurium-rich protective layer was thermally removed from the surface, a pristine zincblende CdTe surface is obtained. In bulk form, the α-Sn phase is stable at temperatures below about 14 °C. To enhance the growth of the diamond cubic α-Sn phase, the thermally cleaned CdTe substrates were cooled to the unusually low growth temperature of 253 K (–20 °C). The tin source material was heated in a standard MBE effusion cell to obtain a tin molecular beam that has a deposition rate of 0.04 μm/h. MBE growth was initiated on the pristine CdTe at 253 K by opening the shutter and directing the molecular beam of tin at the CdTe substrate. Successful epitaxial growth was confirmed by the obtained diffraction pattern using reflection-high-energy-electron-diffraction (RHEED), as shown on the right panel of Fig. 1. Although MBE growth of α-Sn has been previously been reported for (001) CdTe, this is the first demonstration of (111) MBE growth on (111) CdTe.[7]

A Witec alpha 300a spectrometer was used to detect the Raman scattering spectra with resolution of 0.9 cm^{-1} at 300 K in the backscattering geometry using a 1-mW, 532-nm laser. An incident laser power of 1 mW and a measurement time of 10 s was used to avoid sample heating. The α-Sn layers were also characterized with high-resolution X-ray diffraction, Hall, and atomic force microscopy (AFM) measurements.

Approved for public release; distribution unlimited.

3. Results

The high-resolution X-ray diffraction spectrum of the epitaxial α-Sn/CdTe (111) is presented in Fig. 2. The thickness of the epitaxial layer is 20 nm. There are several important points that are indicated:

1) The spacing between the (111) diffraction peaks of α-Sn and CdTe is 0.026. This is evidence for very small strain between the α-Sn epitaxial layer and the CdTe substrate. The unstrained lattice parameter for CdTe is 0.6482 nm and the unstrained lattice parameter for α-Sn is 0.6489 nm. Assuming zero strain and using the respective (111) reflections of the unstrained materials, the predicted difference between the peaks should be 0.027, which is within experimental error of the experimental observation.

2) There appears to be an ultra-thin interdiffused alloy layer of $(\alpha\text{-Sn})_x(SnTe)_{1-x}$. The evidence that supports that is shown as the small diffraction peak at a slightly larger diffraction angle of 23.75°. Tin-telluride (SnTe) has an unstrained lattice constant of 0.630 nm. If the SnTe were pure, the position of the (111) diffraction peak should be located at 24.44°. Also, if there was a pure, coherently strained layer, it would be in a strongly tensile state of strain, which would cause the Bragg diffraction peak to shift to even larger than 24.44°. Because the peak is broad and shifter to a smaller angle, this indicates an expansion of the lattice, which is likely caused by the formation of an alloy of SnTe with α-Sn whose lattice constant is larger. The formation and presence of this alloy layer can be explained by the presence of adventitious Te that resides on the surface after thermal cleaning of the CdTe substrate under a Te overpressure. Because the intensity is more than 2 orders of magnitude weaker than the main Bragg peaks, the layer must be ultra-thin with respect to the thickness of the α-Sn, and likely has thickness on the scale of monolayers, approximately 1 nm.

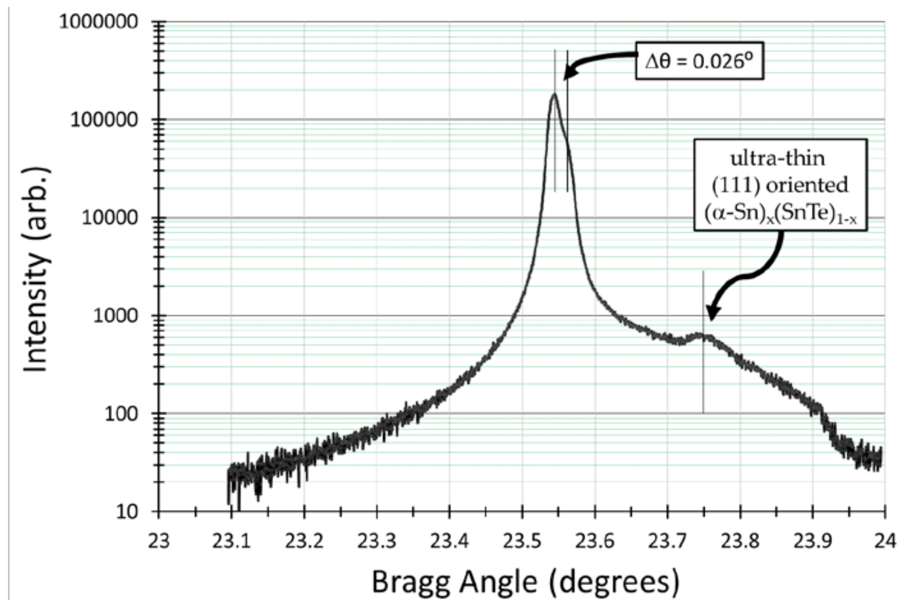

Fig. 2 X-ray diffraction spectrum from 20-nm-thick epitaxial α-Sn/CdTe (111)

Preliminary Hall effect measurements indicate that the α-Sn layers are p-type with a hole concentration of 2×10^{18} cm^{-3} and a mobility of 400 cm^2/Vs. Micron-scale photographs of the surface of a 1000- and 200-Å MBE-grown layer of α-Sn obtained using a 100× microscope lens are shown in Fig. 3. Triangular-shaped etch pits from the etched CdTe substrates are observed in both surfaces. The size and density of these etch pit defects depends on the quality of the CdTe substrate and the substrate cleaning procedures. These etch pits do not significantly affect the MBE growth of α-Sn. The 1000-Å layer exhibits more CdTe substrate surface roughness and larger etch pits compared to the 200-Å layer, but this does not prevent the heteroepitaxial growth of α-Sn over essentially the entire CdTe buffer layer.

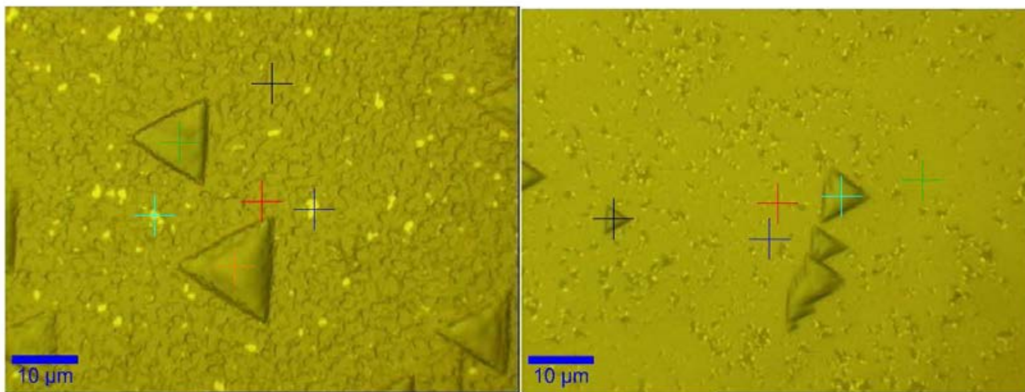

Fig. 3 Photograph of the surface of a 1000-Å (left) and 200-Å (right) layer of α-Sn

Approved for public release; distribution unlimited.

AFM topography maps of the 2 layers confirm that the 200-Å layer shows decreased roughness compared to the 1000-Å layer. The AFM map of the 200-Å layer, shown in Fig. 4, shows regions with peak fluctuations in surface height of around 30 µm surrounded by larger areas with height fluctuations less than 5 µm.

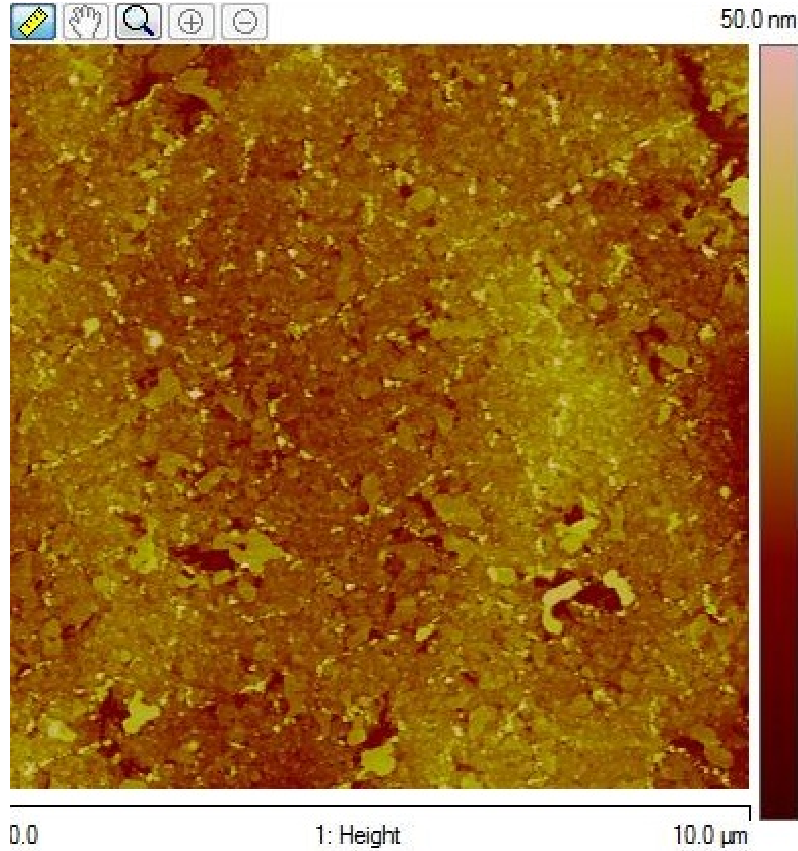

Fig. 4 Color-coded AFM map of the surface of a 200-Å layer of α-Sn

Raman scattering spectra from different points on a 1000-Å layer of α-Sn are shown in Fig. 5. The color of the various Raman spectra in Fig. 5 corresponds with the color of the crosses in Fig. 3, which indicate the position of the incident laser light. We observe a prominent Raman scattering signal at 197.3 cm^{-1} at several measurement points on the 1000-Å layer of α-Sn, which agrees with previous results[8,11] and confirms the growth of slightly strained epitaxial α-S on the CdTe buffer layer. The lineshape of the Raman signal for the 1000-Å layer of α-Sn is nearly symmetrical with respect to the peak energy and its full width at half maximum (FWHM) is constant across the layer at approximately 9 cm^{-1}. The Raman scattering signal from the bright spot on the 1000-Å layer of α-Sn, denoted by the blue cross in Fig. 3, is shown by the blue plot in Fig. 5. The data from the bright spot show the absence of the 197.3-cm^{-1} α-Sn Raman peak, a reduced

background, and a Raman signal with peak energy at 128 cm^{-1}, which is attributed to tin oxide. Since the Raman scattering measurements are carried out on the as-grown unpolished samples, the background signal due to diffuse Raleigh scattering from the surface varies with the surface roughness.

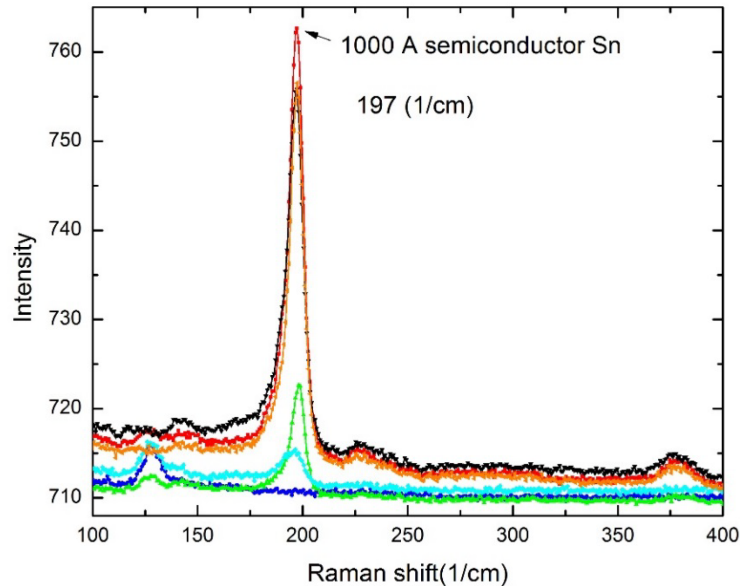

Fig. 5 Raman scattering spectra from a 1000-Å layer of α-Sn

The absence of the 197.3-cm^{-1} Raman peak and the reduced background signal from the bright spot confirms that the tiny bright spots on the 1000-Å layer of α-Sn are metallic, β-Sn. The Raman scattering spectrum from the 200-Å layer of α-Sn, shown in Fig. 6, exhibits a peak energy at 196.5 cm^{-1}, a broadened asymmetrical lineshape with a FWHM equal to 14 cm^{-1}. The data clearly show that the 200-Å layer of α-Sn is epitaxial even though the mechanism for the decrease in peak energy and the increased linewidth are still under investigation. The data in Fig. 6 also show that the 200-Å layer of α-Sn facilitates observation of a larger CdTe longitudinal mode phonon Raman scattering signal at 141.7 cm^{-1} from the underlying CdTe buffer layer. Density functional theory calculations of the Raman scattering peak energy for bulk α-Sn show good agreement with the experimental results.

Approved for public release; distribution unlimited.

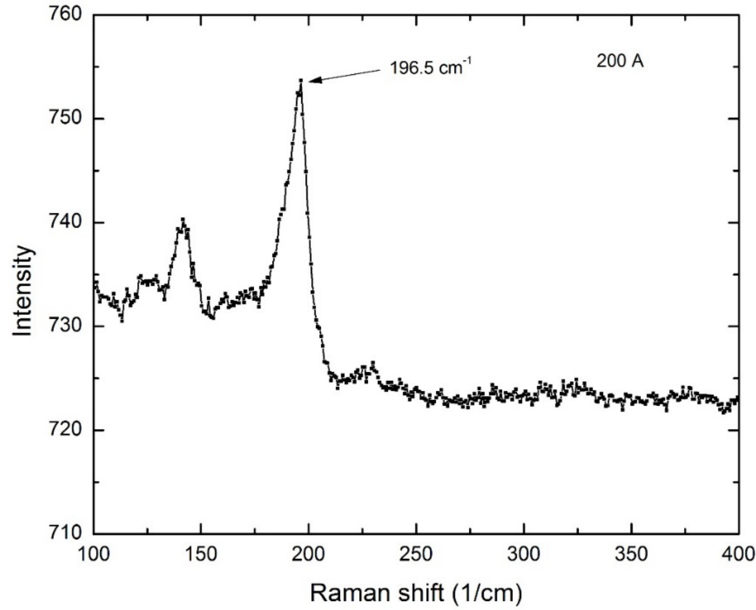

Fig. 6 Raman scattering spectrum from a 200-Å layer of α-Sn

4. Conclusion

Thin layers of single-crystal epitaxial semiconductor α-Sn were grown by MBE on CdTe substrates. X-ray diffraction and Raman scattering measurements confirm that the thin layers of α-Sn are slightly strained, which supports theoretical predictions that α-Sn is a 3-D TI. Future studies will aim at the growth of α-Sn with improved transport characteristics using high-quality CdTe buffer layers, studies of the 3-D TI characteristics of α-Sn, and the MBE growth of stanene.

Approved for public release; distribution unlimited.

5. References

1. Hasan MZ, Kane CL. Rev Mod Phys. 2010;82:3045.
2. Chen YP. Proc SPIE 2012;(8373):83730B.
3. Xu Y, Yan B, Zhang H-J, Wang J, Xu G, Tang P, Duan W, Zhang S-C. Phys Rev Lett. 2013;111:136804.
4. Price DL, Rowe JM. Solid State Comm. 1969;7:1433.
5. Fu L, Kane CL. Phys Rev B. 2007;76:045302.
6. Barfuss A, et al. Phys Rev Lett. 2013;111:157205.
7. Farrow RF, et al. J Cryst Growth. 1981;54:507.
8. Buchenauer CJ, Cardona M, Pollak FH. Phys Rev B. (1971);3:1243.
9. Iliev M, Sinyukov M, Cardona M. Phys Rev B. 1977;12:5350.
10. Kotinadeb I, et al. Semicond Sci Technol. 1998;13:890.
11. Menendez J, Hochst H. Thin Solid Films. 1984;111:375.

Approved for public release; distribution unlimited.

List of Symbols, Abbreviations, and Acronyms

2-D	2-dimensional
3-D	3-dimensional
AFM	atomic force microscopy
CdTe	cadmium telluride
FWHM	full width at half maximum
RHEED	reflection-high-energy-electron-diffraction
SnTe	tin-telluride
Te_2	tellurium dimers
TI	topological insulator
α-Sn	semiconductor tin

1 (PDF)	DEFENSE TECH INFO CTR DTIC OCA
2 (PDF)	US ARMY RSRCH LAB IMAL HRA MAIL & RECORDS MGMT RDRL CIO L TECHL LIB
1 (PDF)	GOVT PRNTG OFC A MALHOTRA
12 (PDF)	US ARMY RSRCH LAB RDRL SED C C RONG RDRL SED E C M WAITS H HIER K A JONES N JANKOWSKI P BARNES P FOLKES P TAYLOR RDRL SED E SHAFFER RDRL SER L B NICHOLS M DUBEY RDRL WMM G M NEUPANE

Approved for public release; distribution unlimited.